30.3 Organic-Transistor-Based 2kV ESD-Tolerant Flexible Wet Sensor Sheet for Biomedical Applications with Wireless Power and Data Transmission Using 13.56MHz Magnetic Resonance

Hiroshi Fuketa[1,2], Kazuaki Yoshioka[1,2], Tomoyuki Yokota[1,2], Wakako Yukita[1,2], Mari Koizumi[1,2], Masaki Sekino[1,2], Tsuyoshi Sekitani[1,2], Makoto Takamiya[1,2], Takao Someya[1,2], Takayasu Sakurai[1,2]

[1]University of Tokyo, Tokyo, Japan, [2]JST/ERATO, Tokyo, Japan

A wet sensor, which detects the presence or absence of liquid, is an important tool for biomedical, nursing-care, and elderly-care applications such as the detection of blood in bandages, sweat in underwear, and urination in diapers. A wet sensor should be a thin, mechanically flexible, large-area, and low-cost device with wireless power and data transmission, because constant monitoring with a rigid and wired wet sensor placed on human skin is annoying. Moreover, the wet sensor should be disposable from a hygiene perspective. In order to meet these requirements, an organic transistor based flexible wet sensor sheet (FWSS) with wireless power and data transmission using 13.56MHz magnetic resonance is developed to detect urination in diapers.

Figure 30.3.1 shows a photograph of the developed 78mm x 53mm FWSS. In its actual implementation, the FWSS is embedded in the cotton of a diaper, although FWSS is placed on the surface of the diaper in Fig. 30.3.1 for clarity. The FWSS is a passive transponder that is wirelessly powered by a reader and sends sensor data to the reader. In the FWSS, organic circuits fabricated on a 12.5μm-thick flexible polyimide film are stacked on 40mm square coil on 12.5μm-thick flexible PCB.

Figure 30.3.2 (a) shows a circuit schematic of the FWSS and reader. The reader is expected to be attached to the pants near the diaper. The reader wirelessly transmits power between the coils (L_1 and L_2) via magnetic resonance at 13.56MHz. In this work, instead of conventional electromagnetic induction [1,2], magnetic resonance is used to increase the distance between the reader and FWSS. The typical power supply voltage (V_{DD}) of the FWSS is 2V. In the FWSS, except for L_2 shown in Fig. 30.3.1, all the circuits including capacitors are integrated in the organic transistor film. In the FWSS, the resistance between two electrodes is measured to detect the presence or absence of liquid. Actually, the resistance is converted to the frequency of TXdata by an RC oscillator (Fig. 30.3.4) in the wet sensor. Then, TXdata performs the load modulation in the transponder and the demodulated signal is RXdata. Fig. 30.3.2 (b) shows the measured waveforms of V_2 and TXdata in the FWSS and RXdata in the reader. The 10Hz frequency of TXdata is successfully demodulated in the reader.

The design challenges of the FWSS are as follows. 1) The power consumption of the battery-operated reader is large because the reader must transmit a maximum power to deal with the loss of transmission efficiency due to the bending of the flexible coil (L_2) as well as change in the distance between L_1 and L_2. 2) ESD protection is essential in the FWSS because the electrodes can directly come in contact with wet human skin. ESD protection in organic transistors, however, is difficult because they are fabricated on an insulating film. To solve these problems, we propose the following two solutions. 1) Adaptive amplitude control (AAC) decreases the power consumption of the reader by reducing the amplitude by up to 92%. 2) ESD protection circuits with organic Schottky diodes using copper phthalocyanine (CuPc) are used to achieve 2kV ESD tolerance. Both AAC and ESD protection are essential technologies in wireless and flexible sensors for biomedical and elderly-care applications.

Figure 30.3.3(a) shows a circuit schematic of the wet sensor, including a four-input multiplexer and three RC oscillators. The four inputs are toggled with a preamble for the data receiver in the reader. The reference RC oscillator is used in the proposed AAC and the other two RC oscillators are used as the wet sensors. In AAC, as shown in Fig. 30.3.2 (a), the amplitude of the reader (V_1) is adaptively controlled by the adaptive amplitude controller to maintain the frequency of the reference oscillator at a target value, which regulates V_{DD} of the FWSS. Figures 30.3.3(b) and (c) show a circuit schematic and a photograph of the four-input multiplexer based on a pseudo-CMOS [3], respectively. The pseudo-CMOS is used to obtain a high gain in pMOS-only organic transistors. To demonstrate the multiplexer, Fig. 30.3.3(d) shows measured waveforms of TXdata, RC oscillator 3, and the reference RC oscillator 1. In this measurement, the reference RC oscillator 1 is 10Hz, RC oscillator 2 (= Sensor 1) is not oscillating, which corresponds to "Dry" (= no urination), and RC oscillator 3 (= Sensor 2) is 5Hz, which corresponds to "Wet" (= urination). Figure 30.3.3(d) shows a successful toggle operation of the multiplexer.

Figure 30.3.4(a) shows a circuit schematic of the RC oscillator with the pseudo-CMOS inverters [3]. The RC oscillator converts the resistance between electrodes (R_{MEA}) to the frequency of OSC. Fig. 30.3.4 (b) shows the measured waveform of OSC. Figure 30.3.4(c) shows the measured dependence of the oscillation period on R_{MEA}. In this work, the target range of R_{MEA} is from 2MΩ to 10MΩ because R_{MEA} in cotton immersed in normal saline is several megaohms. The oscillation period linearly depends on R_{MEA} with an offset. The sensitivity of the resistance sensor is 3.5%/MΩ, though such sensitivity is not required in the FWSS which detects the presence or absence of liquid.

In Fig. 30.3.5, the change in the transmission efficiency due to the bending of the flexible coil (L_2) as well as the changes in distance between L_1 and L_2 is discussed. Figure 30.3.5(a) shows the measurement setup used to investigate the relationship between the input voltage (V_{IN}) in the reader and the output voltage (V_{OUT}) in the FWSS. The bending (B) of the flexible coil (L_2) and the distance (D) between L_1 and L_2 are varied. Figure 30.3.5(b) shows a photograph of the coil L_1 and the bent coil L_2. Figure 30.3.5(c) shows the measured D dependence of V_{IN}/V_{OUT} at B of 0mm and 17mm. D of 40mm is equal to the diameter of L_1 and L_2. The required V_{OUT} for the FWSS is constant. Therefore, V_{IN} should be increased as D and B increase. In the conventional design, a constant V_{IN} (= 9.7 x V_{OUT}) is used to guarantee the required V_{OUT} in the worst case of D=40mm and B=17mm. A constant V_{IN}, however, is usually a waste of the energy, because the required V_{IN} is smaller than 9.7 x V_{OUT} in most cases, as shown in Figure 30.3.5(c). Therefore, AAC is proposed to track the minimum V_{IN}, which reduces the power consumption of the battery-operated reader. AAC reduces V_{IN} by up to 92%. To clarify the effect of B on V_{IN}, Figure 30.3.5(d) shows the measured D dependence of V_{IN} at B=17mm / V_{IN} at B=0mm extracted from Fig. 30.3.5(c). By changing B from 0mm to 17mm, V_{IN} should be increased by a factor of more than 1.5 when D is larger than 10mm. Therefore, AAC is more effective in applications where the coil is bent.

Figure 30.3.6(a) shows a schematic of the circuit developed for ESD protection. Instead of an organic pMOSFET, a vertical organic Schottky diode [4] is used as the diode for ESD as well as a rectifier, because the Schottky diode has large current drivability and a superior frequency characteristic compared with a MOSFET. Figures 30.3.6(b) and (c) show a cross section and a photograph of the organic Schottky diode using CuPc, respectively. The ESD tolerance is evaluated in accordance with the ESD standard IEC 61000-4-2 with a MiniZap ESD simulator [5]. Figure 30.3.6(d) shows the ESD measurement steps and the measured results. Without the ESD protection, the ESD tolerance is below 0.5kV. In contrast, with the ESD protection, the ESD tolerance is above 2kV, which successfully satisfies level 1 of IEC 61000-4-2. One of the issues of adding ESD protection to the signal pad is bandwidth degradation. Figure 30.3.6(e) shows the measured frequency dependence of the gain of the source follower with and without the ESD protection. By adding the ESD protection, the -3dB bandwidth is reduced from 500Hz to 300Hz, which is not a problem in the FWSS because the oscillation frequency is less than 4Hz, as shown in Fig.30.3.4(c). Figure 30.3.7 shows a micrograph of the organic full-wave rectifier and RC oscillator, and a summary of key features.

References:

[1] L. Yan, et al., "A 3.9mW 25-Electrode Reconfigured Thoracic Impedance/ECG SoC with Body-Channel Transponder," *ISSCC Dig. of Tech. Papers*, pp. 490-491, Feb. 2010.

[2] J. Yoo, et al., "A 5.2mW Self-Configured Wearable Body Sensor Network Controller and a 12μW 54.9% Efficiency Wirelessly Powered Sensor for Continuous Health Monitoring System," *ISSCC Dig. of Tech. Papers*, pp. 290-291, Feb. 2009.

[3] K. Ishida, et al.,"Insole Pedometer With Piezoelectric Energy Harvester and 2V Organic Digital and Analog Circuits," *ISSCC Dig. of Tech. Papers*, pp. 308-309, Feb. 2012.

[4] Y. Ai, et al., "14 MHz Organic Diodes Fabricated Using Photolithographic Processes," Appl. Phys. Lett. 90, 262105 (2007).

[5] Thermo Scientific, MiniZap ESD tester, Accessed Sep. 2013, <https://static.thermoscientific.com/images/D20078~.pdf>.

 978-1-4799-0920-9/14/$31.00

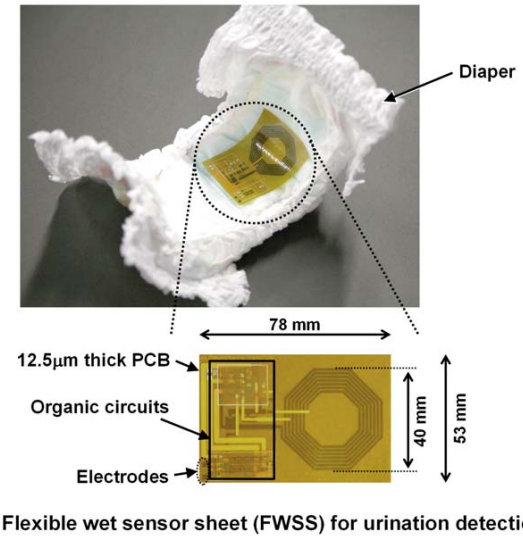

Figure 30.3.1: Developed flexible wet sensor sheet (FWSS).

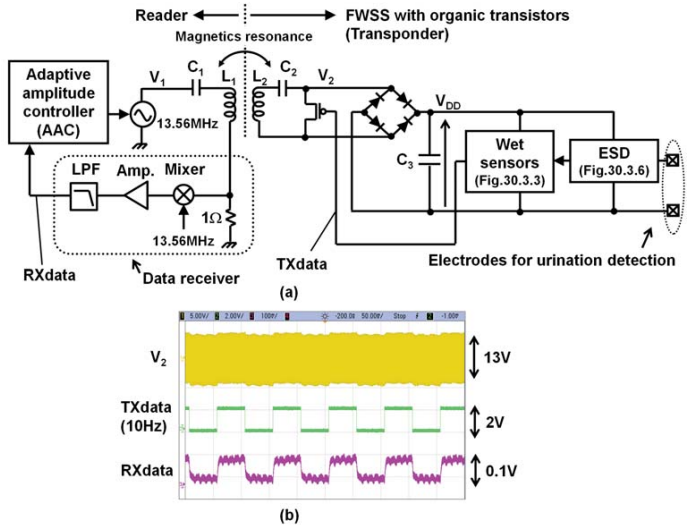

Figure 30.3.2: (a) Circuit schematic of FWSS and reader. (b) Measured waveforms of load modulation.

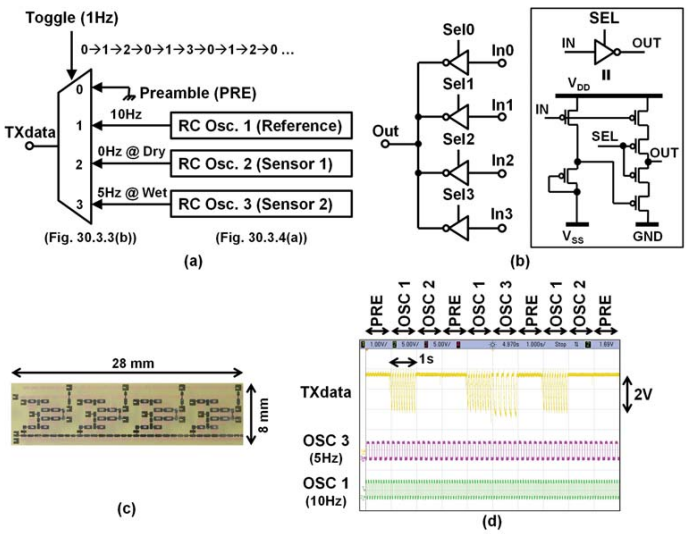

Figure 30.3.3: (a) Circuit schematic of wet sensor. (b) Circuit schematic, (c) photograph, and (d) measured waveforms of four-input multiplexer.

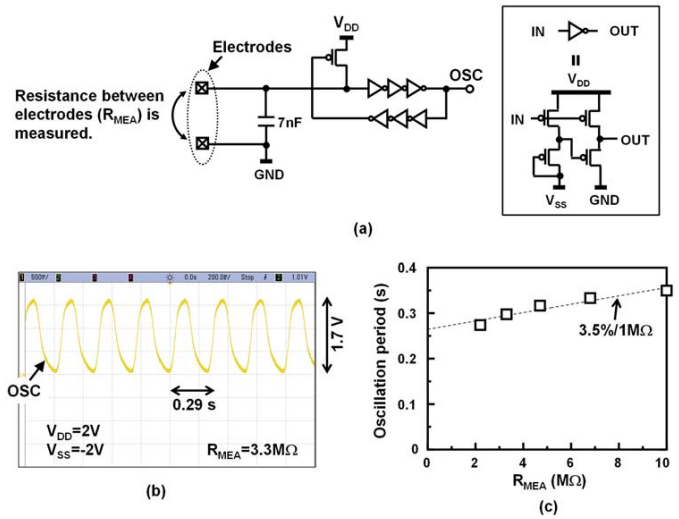

Figure 30.3.4: RC oscillator. (a) Circuit schematic. (b) Measured waveform. (c) Measured dependence of oscillation period on R_{MEA}.

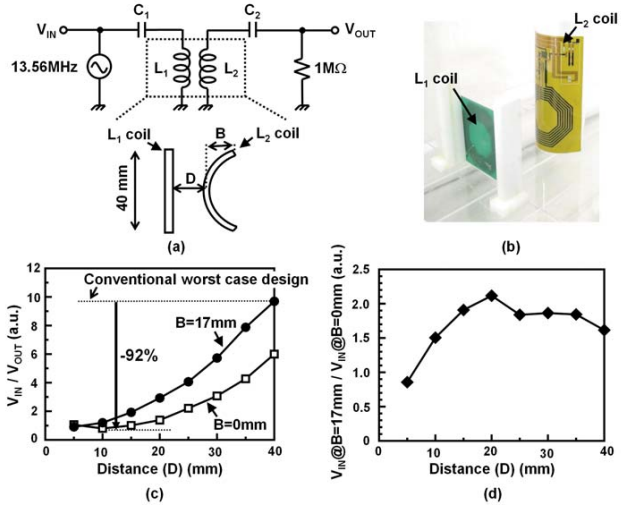

Figure 30.3.5: Bending of flexible coil (L_2). (a) Measurement setup. (b) Photograph. (c) Measured D dependence of V_{IN}/V_{OUT}. (d) Measured D dependence of V_{IN} at B=17mm / V_{IN} at B=0mm.

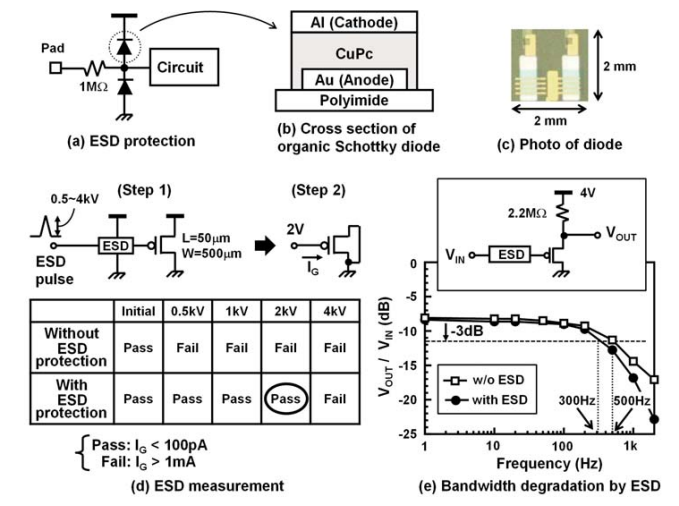

Figure 30.3.6: ESD protection. (a) Circuit schematic. (b) Cross section and (c) photograph of organic diode. (d) ESD measurement. (e) Bandwidth degradation caused by ESD protection.

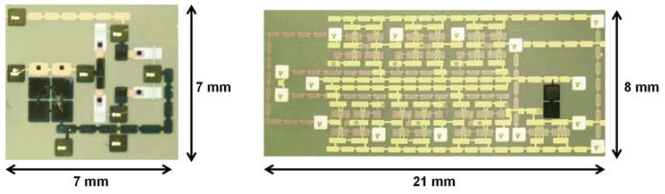

(a) Full wave rectifier (b) RC oscillator

Organic transistors	
Semiconductor material	DNTT(1.0 cm^2/Vs)
Gate insulator, thickness	Parylene 70~80nm
Minimum gate length	50μm
Organic diode	
Material	CuPc
RC oscillator	
Power dissipation	1.4μW @ 2V, 3Hz
Number of Transistors	25

Figure 30.3.7: Micrographs and key features.

978-1-4799-0920-9/14/$31.00